J Neurophysiol 98: 3600–3613, 2007.
First published October 3, 2007; doi:10.1152/jn.00121.2007.

Separate Adaptive Mechanisms for Controlling Trajectory and Final Position in Reaching

Robert A. Scheidt[1,2,3] and Claude Ghez[4]

[1]*Department of Biomedical Engineering, Marquette University, Milwaukee, Wisconsin;* [2]*Department of Physical Medicine and Rehabilitation, Feinberg School of Medicine, Northwestern University;* [3]*Sensory Motor Performance Program, Rehabilitation Institute of Chicago, Chicago, Illinois; and* [4]*Columbia University Medical Center, New York, New York*

Submitted 3 August 2006; accepted in final form 28 September 2007

Scheidt RA, Ghez C. Separate adaptive mechanisms for controlling trajectory and final position in reaching. *J Neurophysiol* 98: 3600–3613, 2007. First published October 3, 2007; doi:10.1152/jn.00121.2007. We examined control of the hand's trajectory (direction and shape) and final equilibrium position in horizontal planar arm movements by quantifying transfer of learned visuomotor rotations between two tasks that required aiming the hand to the same spatial targets. In a trajectory-reversal task ("slicing"), the hand reversed direction within the target and returned to the origin. In a positioning task ("reaching"), subjects moved the hand to the target and held it there; cursor feedback was provided only after movement ended to isolate learning of final position from trajectory direction. We asked whether learning acquired in one task would transfer to the other. Transfer would suggest that the hand's entire trajectory, including its endpoint, was controlled using a common spatial plan. Instead we found minimal transfer, suggesting that the brain used different representations of target position to specify the hand's initial trajectory and its final stabilized position. We also observed asymmetrical practice effects on hand trajectory, including systematic curvature of reaches made after rotation training and hypermetria of untrained slice reversals after reach training. These are difficult to explain with a unified control model, but were replicated in computer simulations that specified the hand's initial trajectory and its final equilibrium position. Our results suggest that the brain uses different mechanisms to plan the hand's initial trajectory and final position in point-to-point movements, that it implements these control actions sequentially, and that trajectory planning does not account for specific impedance values to be implemented about the final stabilized posture.

INTRODUCTION

Reaching to grasp a pint of Guinness requires accuracy in transporting the hand and precision in specifying its final position. Limb compliance at the time of contact also needs to be specified appropriately to avoid upsetting the glass (and its intended recipient) if the exact location is misestimated. In natural tasks, demands for controlling the hand's spatial trajectory, endpoint position, and compliance vary widely in different contexts. The demonstration in primates that specialized cortical neurons are recruited for movement and posture control (Humphrey 1983; Kurtzer et al. 2005) introduces the possibility that the CNS may implement separate spatial plans for the control of hand movement and its final position. This idea would contradict the widely accepted view that a unified kinematic plan governs and constrains movement trajectory and final stabilized arm position during goal-directed reaching (Feldman 1966, 1986; Flash 1987; Flash and Hogan 1985; Gribble and Ostry 1998, 2000; Harris and Wolpert 1998).

Unified kinematic planning in point-to-point movements has been supported by a variety of studies demonstrating that feedforward commands are adapted to maintain handpath rectilinearity and endpoint accuracy in response to environmental perturbations and distortions of visual feedback. However, some experiments have shown that errors induced during and at the end of movement may be compensated differentially, suggesting staggered feedforward specification of initial movement trajectory and final position (Dizio and Lackner 1995; Sainburg et al. 1999). Consistent with this, a recent imaging study has implicated distinct neural systems for moment-by-moment error processing as required in feedback stabilization of hand position and for error processing on a much longer timescale as required for feedforward adjustments to the feedback controller set point (Suminski et al. 2007).

The present experiments asked whether different mechanisms are used to control movement trajectories and final positions. To address this question we examined the transfer of learned visuomotor rotations between two tasks that required subjects to aim the hand to the same spatial locations. The tasks differed in terms of the movement feature that subjects were instructed to control. In a trajectory-reversal task (*slicing*), subjects were to move out-and-back to transiently acquire the target as the hand reversed direction. In a positioning task (*reaching*), they were to move their hand to the target and maintain it there. Separate groups of subjects learned the visuomotor rotation while performing one or the other of the two tasks. We identified the spatial locations learned in each case by examining performance in test trials of both types made without visual feedback. If subjects used the same spatial representation to aim their hand in the two tasks, learning achieved in one should transfer to the other. Alternatively, if subjects used different spatial representations, learning achieved in one task should not transfer to the other. Two sets of experiments examined the effects of varied stabilization requirements and visual feedback signals.

We found minimal transfer of learning for trajectory reversals and stabilized positions in both experiments, suggesting that subjects had adapted different spatial representations of target location in the two tasks. We also observed unexpected changes in hand trajectories during learning and transfer. In

Address for reprint requests and other correspondence: R. A. Scheidt, Department of Biomedical Engineering, Olin Engineering Center, 303, P.O. Box 1881, Marquette University, Milwaukee, WI 53201-1881 (E-mail: scheidt@ieee.org).

The costs of publication of this article were defrayed in part by the payment of page charges. The article must therefore be hereby marked "*advertisement*" in accordance with 18 U.S.C. Section 1734 solely to indicate this fact.

particular, hand path curvature increased during learning and transfer of reaching, but not during slicing, whereas slices became hypermetric after reach training. These observations were not consistent with the application of different, task-dependent strategies in the two cases. Rather, these experimental findings were predicted by a computational model using separate and sequential feedforward control of initial movement direction and final stabilized limb configuration. Portions of this work were previously presented in abstract form (Scheidt and Ghez 2006a,b; Scheidt et al. 2004).

METHODS

Sixteen neurologically normal subjects (ages 21 to 67 yr; 12 male and 4 female) provided written, informed consent to participate in these experiments conducted at the Rehabilitation Institute of Chicago. Study procedures and consent forms were institutionally approved in accord with the Declaration of Helsinki. Subjects were seated in a high-backed chair and a chest harness minimized trunk movement. Subjects moved the instrumented handle of a horizontal planar robot (Scheidt et al. 2001) with their dominant hand (15 = right, 1 = left) between targets projected onto an opaque screen immediately above the plane of movement. The subject's arm was supported against gravity (between 75 and 90° abduction angle) using a lightweight, chair-mounted arm support. A drape covering the shoulder and upper arm prevented subjects from seeing their hand and arm. Upper arm and forearm segment lengths were measured in each subject as was the shoulder center of rotation relative to the origin of the robot's workspace.

Tasks

This report describes two sets of experiments. Each required subjects to perform two motor tasks. A trajectory-reversal task (*slicing*) required subjects to move to one of eight equidistant (15 cm) circular targets (2-cm diameter) where they were to reverse direction without pausing. They were then to return the hand to the origin and stabilize it there. Targets and starting positions were oriented such that movements away from and toward the body (90 and 270°) were directed along the midclavicular line on the subject's dominant side. Target directions were randomized across trials. A positioning task (*reaching*) required subjects to move the hand from the same starting position to the same target locations and to hold it there a period of time (see following text). The manipulandum then moved the hand passively back to the starting position. Subjects were instructed to achieve a peak hand speed of 0.5 m/s across trials and tasks and were provided with a bar graph display of the peak velocity after each trial to assist them in doing so. In the second experiment, an augmented display of velocity information (described in the following text) was used to encourage tighter control of peak velocity.

The first experiment was designed to determine whether learning of initial movement trajectories and intended final positions could be isolated experimentally. Learning of a 30° visuomotor rotation was induced by gradually rotating cursor feedback around the hand's initial position as subjects practiced exclusively on one or the other task (Fig. 1, *A–D*). As subsequently described, we provided cursor feedback (spatial error information) only after the movement had ended during reach training, whereas the cursor was visible throughout movement during slice training. This was done to explore potential differences in the effect of visual feedback on the initial and terminal phases of arm movements. Because this dissimilarity in feedback also provided information that subjects might use to alter their control strategy early in the trajectory, the second experiment was designed to eliminate this and other potential confounds. We assessed learning and transfer to the untrained task in both experiments using test trials made entirely without visual feedback (i.e., those we call "blind" test trials). Data analysis was the same for the two experiments.

Experiment 1

Eleven subjects participated in this experiment. Experimental sessions consisted of three blocks of trials. During the first block (baseline: 192 trials) subjects practiced equal numbers of reaching and slicing trials without rotation. These trials were performed in "cycles" of eight movements each (one trial for each pseudorandomized target direction), with the cycles alternating by task type. During the second block (training), one group of subjects ($n = 6$) practiced only the slicing task whereas the remaining subjects practiced the reaching task. Cursor motion was rotated counterclockwise around the home target incrementally (7.5° every 40 trials) to a maximum of 30°. Learning was generally achieved in 192 trials but some subjects required up to 384. During a third block (test: 192 trials), we assessed transfer of learning across tasks in blind test trials interspersed pseudorandomly every eight training trials.

SLICING TASK. At trial onset, the subject was to bring the cursor to the starting location (indicated by a + sign). After stabilizing the hand within a 1.0-cm radius of the origin for 1.0 s, a target circle appeared at one of the peripheral locations. The presence of a line connecting the start position to the target cued the subject to move the hand out-and-back, reversing directions within the target. The cursor remained visible throughout the movement, providing feedback of both movement direction and reversal location. Note that rotation-induced errors were minimal while the hand was at rest in the slicing task because the rotation was defined about the hand's starting location, the origin.

REACHING TASK. Subjects again aligned their hand at the starting position for 1.0 s. The cursor was then removed and a peripheral target circle was displayed without the radial line. This cued the subject to bring the hand to the target where it was to be maintained still for 1.5 s without visual feedback. The cursor then reappeared for 1.0 s, and subjects were to correct any terminal error by slowly bringing it to the center of the target. Thus the cursor informed the subjects of deviations between the intended and actual final hand positions, but not of the paths during reaching (as during slicing) nor of the hand's initial position before movement. After 1.0 s of such feedback, the cursor was removed again and the subject was to relax while the robot returned the hand to its starting point.

STABILIZATION. We were concerned that subjects might relax their arms too soon after movement and rely on friction and other uncontrolled properties of the manipulandum to keep their hand in place. Therefore to require active control of hand position at initial and target locations, we applied small force perturbations to the handle whenever hand speed was near zero (<0.1 m/s). These perturbations consisted of unpredictable forces (sum of 2.1- and 3.5-Hz sinusoids in the x and y directions; 3.5 N peak-to-peak; Fig. 1*F*). They were unbiased across directions and were phased in and out smoothly, over a period of 250 ms before the onset and after the termination of movement. Our intent was to induce subjects to cocontract antagonist muscles at the elbow and shoulder joints and, by increasing elbow and shoulder joint impedance during positional stabilization, to facilitate identification of the limb's equilibrium configuration.

We verified that cocontraction was indeed necessary to stabilize the hand in a pilot experiment carried out in two subjects (one of whom participated in *experiment* 1). We recorded surface EMGs (Delsys DE-2.1 electrodes and Delsys Bagnolli 8 system; Delsys, Taunton, MA) at 1,000 Hz from an elbow flexor (the short head of the biceps) and an elbow extensor (the lateral head of the triceps). We did so as subjects held their arm at the starting target location for 5 s using graded levels of elbow muscle coactivation. To provide biofeedback of coactivation that subjects could control, the digitized EMGs were

passed through a filter that calculated the instantaneous root-mean-square (RMS) EMG value for each muscle within a sliding, 200-ms time window. At each sampling instant, coactivation $CoA(t)$ was quantified as the minimum of the RMS flexor $F^{RMS}(t)$ or extensor $E^{RMS}(t)$ EMGs represented as a percentile of their individual maximum value EMG_{MAX}^{RMS} recorded during maximal voluntary contraction (MVC) for each muscle (Fig. 1*G*) (cf. Suminski et al. 2007)

$$CoA(t) = \min [F^{RMS}(t), E^{RMS}(t)]$$

This measure does not constrain activation for the more active muscle and allows subjects to control the level of muscle coactivation while maintaining postural stability. Figure 1*H* compares the motions of the handle induced by the perturbation with different levels of coactivation over a 5-s time interval as a subject attempted to maintain the cursor in the target circle. It can be seen that about 10 to 30% coactivation was necessary to maintain the hand within the target circle for most of the time interval.

Experiment 2

This experiment examined whether the differences in hand trajectories and the limited transfer of learning observed in *experiment* 1 resulted from differences in the control of initial trajectory and final position or rather from confounding variables. Possible confounds present in the first experiment included: the presence of a radial line connecting origin to target during slice (but not reach) trials, continuous visibility of the cursor before and during slicing (but not reaching), and the requirement to counter a destabilizing load at peripheral locations in reaching (but only at the starting point in slicing). Thus we made four modifications to the experimental protocol to address these concerns.

First, we used target fill colors rather than a radial line to cue subjects to make slicing (blue) and reaching (red) movements. Second, both slicing and reaching movements were made without continuous cursor feedback. Instead, we provided error information in slicing by displaying the location of the cursor at the reversal point for only 1.0 s (the same duration of feedback as for reaching). The feedback conditions for reaching were as in *experiment* 1. In both cases the hand was placed at the required starting position by the robot without visual feedback. Third, we eliminated the destabilizing hand perturbation. Last, to improve consistency of peak hand speed across tasks, we modified the graphical display of peak hand speed so that it depicted not only the value from the most recent trial, but also values from the previous seven trials. Subjects were encouraged throughout the sessions to center the distribution of peak hand speeds on the desired value of 0.5 m/s.

Five subjects participated in two sessions on separate days (1–7 days apart), adapting to gradually imposed 30° rotations (0.2° per trial) during slice training on one day and during reach training on the other. The order of training sessions was randomized across subjects to minimize the influence of potential order effects. Each session began and ended with the same baseline conditions to wash out aftereffects. The experimental design, including baseline, training, and test blocks, was otherwise as in *experiment* 1.

Data analysis

Instantaneous hand position was recorded at 150 samples/s using 17-bit rotational encoders mounted on the robot's motors. Hand paths (Fig. 1*D*) had a spatial resolution better than 0.2 mm and were low-pass filtered using a second-order, zero-lag Butterworth filter with 20-Hz cutoff frequency before computing hand veloci-

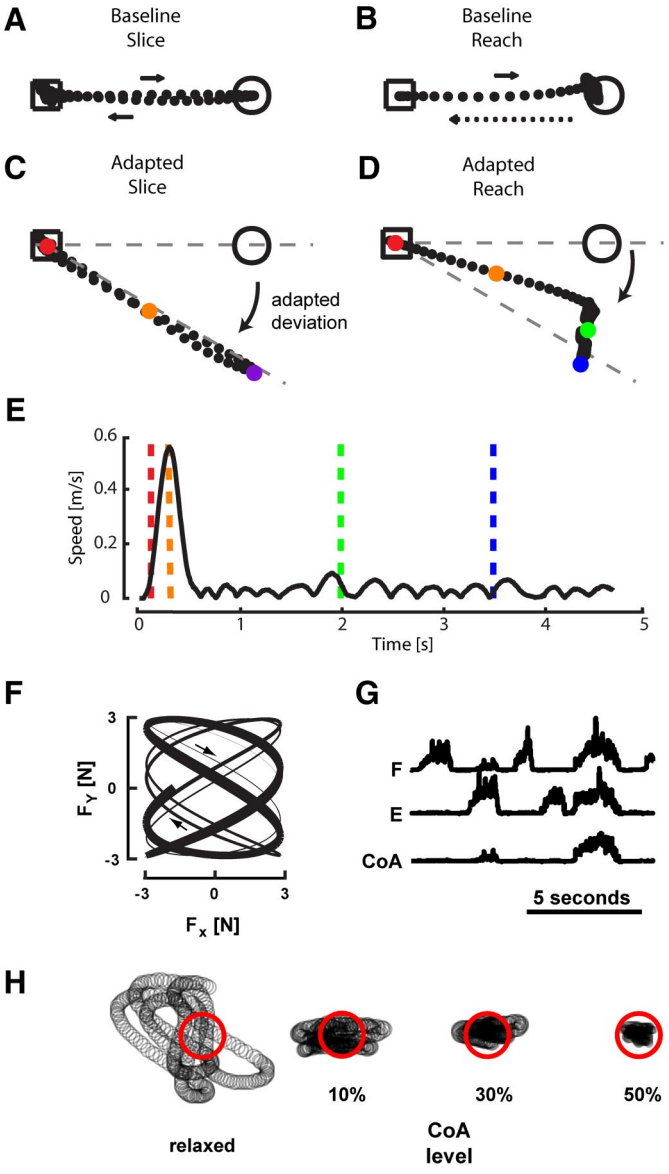

FIG. 1. Schematic description of experimental protocols. *A*: in the aiming task (*slicing*), subjects moved out and back to the target location (open circle), reversing direction within the goal and returning to the starting point (square). *B*: in the positioning task (*reaching*), subjects moved to the target and stabilized the hand there. After a delay, the robot then brought the hand back to its starting point (dotted arrow). *C* and *D*: in both tasks, angular deviation was calculated as the interior angle between a line connecting the start and goal locations and a second line that was defined twice during each movement. Gray dashed lines indicating a 30° rotation about the hand's starting position are shown for illustration purposes only. For slicing movements (*C*), the second vector pointed from the hand's starting location to either the hand's location at the time of peak speed (mid; orange circle) or its reversal point (peak; purple circle). For reaching movements (*D*), the second vector pointed from the hand's starting location to either the hand's location at the time of peak speed (mid; orange circle) or at the end of terminal stabilization without visual feedback (end; green circle). Additional corrections were observed throughout the visual feedback period (blue). *E*: hand speed profile and color-coded vertical markers corresponding to the kinematic features indicated for the positioning trial depicted in *D*. *F*: spatial profile of time-varying hand forces applied by the robot both in *experiment* 1 and in the supporting experiment. Arrows and increasing line thickness indicate the progression of forces in time. *G*: normalized elbow flexor (*F*) and extensor (*E*) activities recorded to demonstrate our measure of elbow flexor/extensor muscle coactivity (CoA). See the text for full details on computation of CoA. *H*: representative hand displacements induced by the hand forces in *F* while the subject was relaxed (i.e., generating no measurable CoA at the elbow; *left*) as well as while CoA was maintained at 10, 30, and 50% of maximum voluntary contraction (from *left* to *right*).

ties (Fig. 1*E*). Velocities were filtered similarly before computing hand accelerations. We identified several kinematic features using an automated algorithm within the MATLAB programming environment (The MathWorks, Natick, MA). Each was verified visually and was manually adjusted if necessary. The hand's *starting point* was defined as its *x–y* location 100 ms before movement onset. Movement onset was identified as the moment when the hand velocity first exceeded 0.1 m/s at the beginning of a trial (Fig. 1, *D* and *E*, red). The *peak acceleration point* consisted of the *x–y* location and peak hand acceleration taken when the hand acceleration reached its maximum positive value in the outward phase of the movement. The *peak speed point* consisted of the *x–y* location and peak hand speed taken when the hand reached its maximum positive speed in the outward phase of the movement (Fig. 1, *D* and *E*, orange). For reaches, the *final position point* (Fig. 1, *D* and *E*, green) consisted of the average *x–y* location over the last 50 data points during terminal stabilization before visual feedback. For slices, we defined the *reversal point* as the *x–y* location taken when the hand reached its maximum radial displacement from the home target in the *outward* phase of the movement (Fig. 1*C*, purple). Because the return phase of slicing movements could also deviate from the intended (home) target, we defined the *return position point* as the *x*–y location taken when the hand reached its maximum radial displacement from the home target during the *return* phase of slicing movements.

We then derived a number of secondary measures to assess the extent of transfer of visuomotor adaptation from one type of movement to the other. Angular deviation was calculated as the interior angle between the desired movement vector in extrinsic space and a second vector that was defined at two points in time for each movement. For slicing movements, this second vector pointed from the hand's starting location to either the hand's location at the time of peak speed (mid; the initial movement direction) or its location at reversal (peak). For reaching, the second vector pointed from the hand's starting location to either its location at the time of peak speed (mid) or to the hand's final position point (end). Thus if a subject had fully adapted to the imposed 30° rotation, then the angular deviation measured at both mid and peak (or end) of movement should equal −30°. We also used these angular deviation measures to compute a proxy of movement curvature [i.e., the difference in angular deviation between peak (or end) and mid movement $d\theta = \theta_{peak(end)} - \theta_{mid}$].

Statistical testing was carried out within the Minitab computing environment (Minitab, State College, PA). Data values are reported as means ±1SD. Error bars in figures also represent ±1SD. Repeated-measures ANOVA and subsequent post hoc tests were used to compare performance measures across training conditions, tasks, and experimental blocks. Effects were considered statistically significant at the $\alpha = 0.05$ level.

Simulations

We performed a set of forward dynamic numerical simulations to explore the behavioral ramifications of separate and sequential feedforward specification of the hand's initial movement direction and the limb's stabilized configuration at the end of movement. We also sought to determine the sensitivity of reach kinematics to varied biomechanical and temporal parameters. We assumed that feedforward specification of the initial limb movement and the location about which the limb would finally be stabilized may be independently adapted by visual feedback of kinematic performance errors as in the experiments described earlier (although we did not attempt to model this adaptation here). As in our psychophysical experiments, we simulated no environmental forces that might perturb the hand from its desired trajectory. Consequently, the hand path kinematics predicted by our simulations result from interaction between separate control mechanisms specifying the hand's initial desired trajectory and the limb's final desired stabilized position.

Three template movements were created within the MATLAB computing environment (The MathWorks). One template was a straight-line reaching movement of 10-cm length and 0.5-s duration. Movement originated from a position 0.4 m in front of the subject and was directed along the midclavicular line (3 cm to the left of the shoulder center of rotation). A second template was composed as the superposition of two, equal and opposite reaches out and back to the same target, directed away from and then toward the body, one delayed by 0.45 s with respect to the other. This composition of trajectory-reversal movements captures the kinematic features of real reversal movements [as also shown by Gottlieb (1998) for single joint motions]. A third template was a reaching movement rotated 30° counterclockwise about the hand's starting location. This template was used to compute the feedforward commands associated with the outward segment of a slicing movement after adapting to the 30° clockwise visuomotor rotation.

Simulation runs were conducted in two phases. First, inverse kinematic calculations were performed to calculate the shoulder and elbow joint angle excursions required to perform each template movement. The shoulder and elbow joint torques required to drive the simulated limb through the template trajectories were calculated using inverse dynamic equations of motion, expressed as

$$\begin{bmatrix} \tau_s \\ \tau_e \end{bmatrix} = \begin{bmatrix} I_s + I_e + m_s r_s^2 + m_e r_e^2 + l_s^2 m_e + 2 l_s m_e r_e \cos(\theta_e) & I_e + m_e r_e^2 + l_s m_e r_e \cos(\theta_e) \\ I_e + m_e r_e^2 + l_s m_e r_e \cos(\theta_e) & I_e + m_e r_e^2 \end{bmatrix} \begin{bmatrix} \ddot{\theta}_s \\ \ddot{\theta}_e \end{bmatrix}$$
$$+ \begin{bmatrix} 0 & -l_s m_e r_e \sin(\theta_e) & -2 l_s m_e r_e \sin(\theta_e) \\ l_s m_e r_e \sin(\theta_e) & 0 & 0 \end{bmatrix} \begin{bmatrix} \dot{\theta}_s^2 \\ \dot{\theta}_e^2 \\ \dot{\theta}_s \dot{\theta}_e \end{bmatrix} + \begin{bmatrix} V_{11} & V_{12} \\ V_{21} & V_{22} \end{bmatrix} \begin{bmatrix} \dot{\theta}_s \\ \dot{\theta}_e \end{bmatrix}$$
$$+ \Phi_R(t) \left[B^* \begin{bmatrix} V_{11} & V_{12} \\ V_{21} & V_{32} \end{bmatrix} \begin{bmatrix} \dot{\theta}_s \\ \dot{\theta}_e \end{bmatrix} - K^* \begin{bmatrix} K_{11} & K_{12} \\ K_{21} & K_{22} \end{bmatrix} \begin{bmatrix} \theta_{s\_reach} & -\theta_s \\ \theta_{e\_reach} & -\theta_e \end{bmatrix} \right]$$
$$+ \Phi_E(t) \left[B^* \begin{bmatrix} V_{11} & V_{12} \\ V_{21} & V_{22} \end{bmatrix} \begin{bmatrix} \dot{\theta}_s \\ \dot{\theta}_e \end{bmatrix} - K^* \begin{bmatrix} K_{11} & K_{12} \\ K_{21} & K_{22} \end{bmatrix} \begin{bmatrix} \theta_{s\_end} & -\theta_s \\ \theta_{e\_end} & -\theta_e \end{bmatrix} \right] \quad (1)$$

Here, the arm was modeled as a two-segment link in the horizontal plane (cf. Scheidt et al. 2005). Each segment was modeled as a homogeneous rigid body with mass **m** concentrated at the center of mass located at distance **r** from the proximal joint. Each segment **i** also had a moment of inertia $\mathbf{I}_i$, where the index **i** = **s** corresponds to the shoulder joint, whereas **i** = **e** corresponds to the elbow joint. This arm model was used to estimate the joint torques needed to drive the arm along the template movements. In our simulations, reaches could potentially be composed as a sequence of two motor commands: one specifying how the limb should transition between initial and final

targets and the other specifying where and how it should be stabilized. Thus the inverse dynamic model we used to compute the joint torques consisted of two parts. The first part (top two lines of *Eq. 1*) computed the torques contributed by a feedforward trajectory controller that we hypothesized should be most influential during the initial phase of reaching movements. We make no assumption regarding how the nervous system generates the feedforward joint torques, whether by modulating motor neuron threshold potentials as in equilibrium trajectory models or by simply specifying a time series of muscle activations. Both approaches would yield the same torques in the absence of environmental perturbations (as was the case here), although they differ in that the equilibrium approach also specifies joint viscoelasticity about a limb position that might or might not be spatially coincident with the desired, final stabilization point (the effects of which are modeled explicitly in the last two lines of *Eq. 1*). This second part of our inverse dynamic model computes the torques contributed by the postural mechanisms stabilizing the hand about two fixed positions in the workspace ($\bar{\theta}_{reach}$ and $\bar{\theta}_{end}$) corresponding to the reach target and origin (i.e., the end/return target), respectively.

The anthropometric parameters used for simulating arm movements for a typical subject were based on previously published simulations of reaching and adaptation to velocity-dependent force fields (Shadmehr and Mussa-Ivaldi 1994) and were modified to attain a limb-damping factor within the physiological range (cf. Perreault et al. 2004). These values were used to define the nominal joint viscoelasticity during movement and in the absence of postural stabilization about $\bar{\theta}_{reach}$ and $\bar{\theta}_{end}$ (Table 1). Although somewhat different values of nominal joint stiffness and viscosity have been reported elsewhere in the literature (cf. Bennett et al. 1992; Perreault et al. 2004), such estimates are not directly applicable to the current simulations because those studies used high-frequency stochastic perturbations to measure limb viscoelasticity, and stochastic perturbations are known to alter joint viscoelasticity through agonist/antagonist muscle cocontraction (Soechting et al. 1981) and, possibly, through the modulation of short-latency reflex activity (cf. Kearney and Hunter 1982).

$\mathbf{\Phi}_{\boldsymbol{R}}(t)$ and $\mathbf{\Phi}_{\boldsymbol{E}}(t)$ represent two sigmoidal functions modeling the time course over which the equilibrium positions (or "posture points") were instantiated at the reach and end/return targets, respectively. Importantly, the simulations assumed that the two posture point locations were fixed in space as a result of extended practice and/or visuomotor adaptation, and that the two multiplicative scaling functions $\mathbf{\Phi}_{\boldsymbol{R}}(t)$ and $\mathbf{\Phi}_{\boldsymbol{E}}(t)$ could take on values ranging continuously from 1 (posture point instantiation) to 0 (no posture point). Based on pilot study findings of similar initial accelerations in reaching and slicing but different peak speeds (Scheidt and Ghez 2006a,b; see also Ghez et al. 2007), the reach and end target posture points were instantiated [i.e., $\mathbf{\Phi}(t) > 0$] at the time of peak acceleration of the outgoing and return phases of the movements, respectively. We also assumed that the equilibrium point at the reach target began turning off 250 ms after onset. It is important to note that the position specified by the controller enforcing limb posture at the end of movement need not be spatially coincident with the endpoint specified by the trajectory controller.

TABLE 1. *Anthropometric and joint mechanical properties used to simulate arm movements*

Parameter	Value
Upper arm length	0.33 m
Upper arm mass	2.62 kg
Upper arm center of mass	0.165 m
Upper arm inertia	0.0231 kg-m^2
Forearm/hand length	0.34 m
Forearm/hand mass	1.52 kg
Forearm/hand center of mass	0.19 m
Forearm/hand inertia	0.0372 kg-m^2
Joint stiffness	$K = \begin{bmatrix} -15 & -6 \\ -6 & -16 \end{bmatrix}$ N-m/rad
Joint viscosity	$V = \begin{bmatrix} -2.1 & -0.8 \\ -0.8 & -2.2 \end{bmatrix}$ N-m-s/rad

Next, we conducted a set of forward dynamic simulations using the computed torques to drive limb motion under altered conditions of postural stabilization. Movements were simulated by propagating the forward dynamic equations of motion (i.e., the inverse of *Eq. 1*) forward in time subject to the torques calculated along the templates. Because the trajectory controller of *Eq. 1* did not require computation of a desired reference trajectory, the temporal influence of the initial trajectory plan was implicitly limited in the forward dynamic simulations, thus yielding a parsimonious implementation of separate and sequential control of the hand's initial movement and its final stabilized position. By setting $\mathbf{\Phi}_{\boldsymbol{R}}(t) = 0$ either in *Eq. 1* or in the forward dynamic equations of motion (but not both), it was possible to simulate errors in planning for the presence or the absence of an equilibrium posture instantiated at the reach target. The underlying assumption here is that, although the trajectory controller achieves nominal trajectories through an error-driven adaptation process, it is not informed of changes in control signals to be generated by the positional controller later in that same movement.

Finally, we assessed the sensitivity of the simulation results to systematic variations in the $\mathbf{\Phi}(t)$ onset timing parameters. Although we initially used values of joint stiffness and viscosity in the physiological range as reported by Lacquaniti et al. (1993) and Gomi and Osu (1998), we systematically explored the effects of varying both stiffness and viscosity within physiological limits during postural stabilization. Evidently, the amount by which these parameters increase during stabilization varies across subjects and levels of cocontraction (Gomi and Osu 1998). We therefore performed multiple simulations, allowing the multiplicative factor scaling joint angular stiffness during stabilization (K*) to increase up to a factor of 2.0. We also allowed the multiplicative factor scaling joint angular viscosity (B*) to increase up to a factor of 3.0.

RESULTS

Adaptation to visuomotor rotations and transfer of learning between conditions

During baseline practice in *experiments* 1 and 2, slices and reaches either reversed direction or terminated near the targets and had the usual rectilinear hand paths (Fig. 2, *left column*) and smooth velocity profiles (cf. Fig. 1*E*). After extended training with the visuomotor rotation, most subjects compensated for the imposed changes in cursor direction with opposite deviations of hand movements both in trained slicing and in trained reaching. The magnitudes of these learned compensatory deviations were approximately the same in both experiments. Because the two experiments revealed similar systematic effects of training condition on slice and reach hand paths as well as on transfer of learning between tasks, we subsequently describe the results from the two experiments together for these subjects, comparing quantitative differences where they occur. Because one subject in *experiment* 1 and two subjects in *experiment* 2 compensated for the imposed rotation during reaching in a qualitatively different manner, results from this group of subjects are presented separately in the following text.

In *experiment* 1, peak velocities were substantially higher in slicing than in reaching movements (0.51 ± 0.11 vs. 0.33 ± 0.09 m/s; $P < 0.001$). We achieved better experimental control over this variable in *experiment* 2 by providing subjects with knowledge of results (KR) of the peak velocities in the previ-

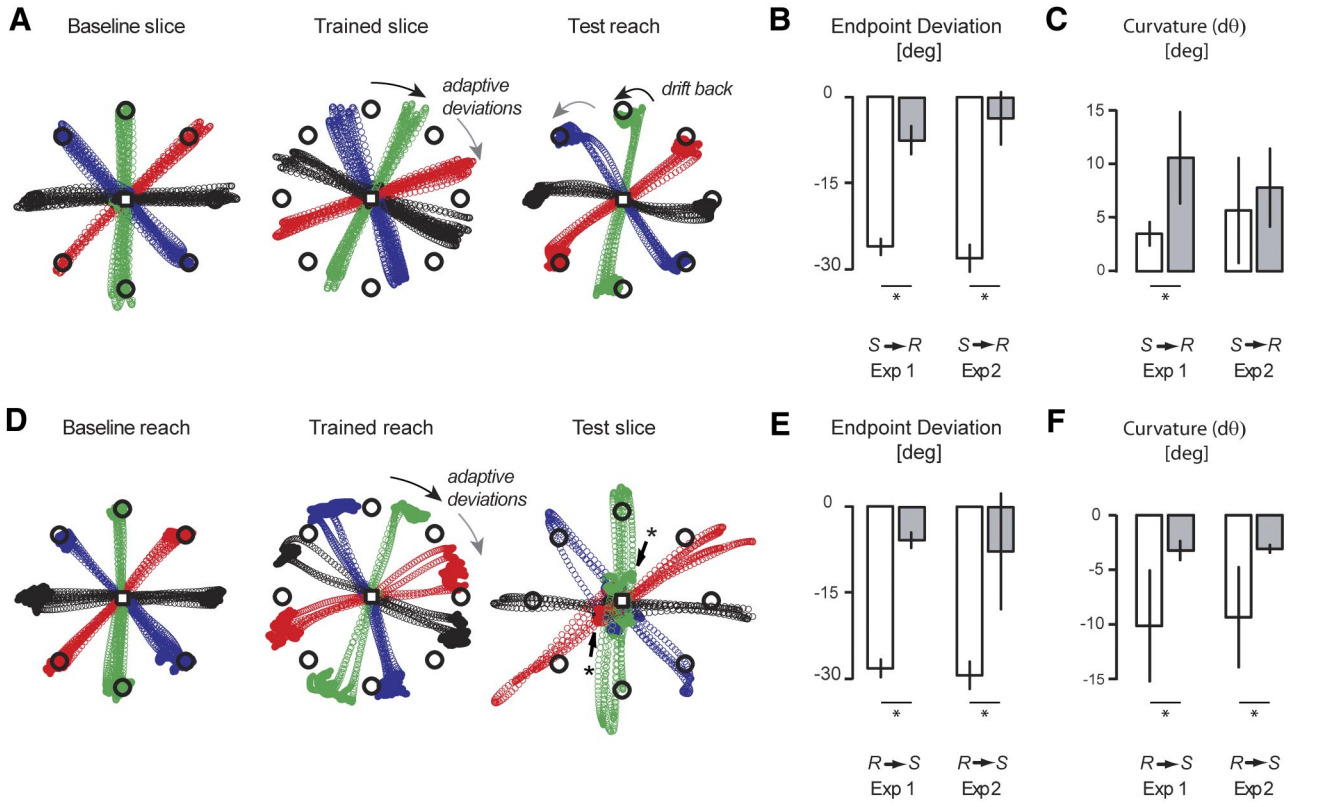

FIG. 2. Incomplete transfer of visuomotor adaptation across trajectory reversal (slicing) and positioning (reaching) tasks. *A*: hand paths of slicing movements under baseline conditions (*left*), after adaptation to 30° counterclockwise (CCW) rotation of the cursor (*middle*; trained slice), and for untrained test reaching movements (*right*) for a representative subject in *experiment* 1. Note that paths of slicing movements before and after training are straight but that test reaches (performed without cursor feedback) initially deviate from baseline directions and drift back toward the unadapted target location at the end of movement. Movement amplitudes of trained slices and test reaches are similar. *B*: angular deviations from the veridical movement direction, averaged across targets and subjects during the last block of slice training. Here and elsewhere, error bars indicate ±1SD, whereas horizontal bars with asterisks indicate statistical comparisons significant at the $P < 0.05$ level. For both *experiment* 1 (*left*) and *experiment* 2 (*right*), deviations of trained slices (S; open bars) came close to the imposed 30° rotation at movement endpoint. For test reaches (R; shaded bars), the hand approached the unadapted (baseline) target location, clearly demonstrating that rotation learning failed to transfer from slice to reach tasks. Although not shown here, transfer of adaptation from slice to reach was greater at midreach than at the end of reach. *C*: difference between angular deviations calculated at the moment of peak hand speed and at the moment of peak displacement (slices) or at the end of stabilization without visual feedback (reaches) after slice training. dθ provides an estimate of hand path curvature. For both *experiment* 1 (*left*) and *experiment* 2 (*right*), reaches were more curved than slices. *D*: hand paths of reaching movements under baseline conditions, after adaptation to 30° CCW rotation of the cursor, and for untrained, blind slicing movements for a representative subject in *experiment* 1. After reach training, initial reach hand paths exhibit limited clockwise deviation, but then bend substantially further away from the original, untrained location at the end of movement. Test slices (performed without cursor feedback) remain straight and minimally deviated from baseline slices (as shown in *A*, *left*). Extents of outward and return strokes of the unadapted test slices are substantially hypermetric (asterisks). *E*: angular deviations from the veridical movement direction, averaged across targets and subjects during the last block of reach training. For both *experiment* 1 (*left*) and *experiment* 2 (*right*), deviations of trained reaches (open bars) came close to the imposed 30° rotation at movement endpoint. For test slices (shaded bars), the hand approached the unadapted (baseline) target location, now demonstrating that rotation learning failed to transfer from reach to slice tasks. *F*: dθ values after reach training again reveal that reaches were more curved than slices in both *experiment* 1 (*left*) and *experiment* 2 (*right*).

ous eight trials (slices: 0.58 ± 0.05 m/s; reaches: 0.54 ± 0.03 m/s), realizing a difference in peak speed during training of only 8 vs. 55% in *experiment* 1. As discussed further in the following text, differences in hand velocity could not account for our observations.

ADAPTATION AND TRANSFER DURING SLICE TRAINING. For all subjects in the slice-trained groups in both experiments, hand paths of slicing movements remained straight during training but were progressively redirected as they learned the visuomotor rotation (Fig. 2*A*; compare *left traces* to the *middle traces* demonstrating clockwise adaptive deviations). The absence of curvature in the trained slices indicates that errors detected during individual movements served to adjust the spatial location toward which subsequent reversals were aimed, rather than to correct movement errors "on-line" (see also Krakauer et al. 2000). In contrast, test reaches made without continuous cursor feedback showed systematic curvatures: Their initial paths were deviated in the clockwise direction (although to a lesser degree than adapted slices), but final positions drifted back toward the unadapted target location (Fig. 2*A*, *right*, drift back). For some trials this occurred before the end of transport, whereas in others it occurred during stabilization (but still without visual feedback).

Across subjects undergoing slice training (Fig. 2*B*), mean adaptive deviations of slices compensated almost fully for the imposed 30° rotation at both midmovement (*experiment* 1: −24.9 ± 1.4°; *experiment* 2: −30.4 ± 5.9°; data not illustrated) and the reversal point (*experiment* 1: −26.1 ± 2.8°; *experiment* 2: −28.1 ± 2.4°). For test reaches, the mean adaptive deviations were also quite large midmovement (*experiment* 1: −16.9 ± 3.5°; *experiment* 2: −10.0 ± 8.7°; data not illustrated), but were much smaller at the end of movement

(*experiment* 1: −7.3 ± 4.9°; *experiment* 2: −3.6 ± 4.6°), approaching baseline values (*experiment* 1: −0.2 ± 1.0°; *experiment* 2: 0.0 ± 1.3°). Hand path curvatures in reaching exceeded those in slicing in *experiment* 1 ($d\theta = 10.5 \pm 4.2°$ vs. 3.5 ± 1.1°; Fig. 2*C*). A similar trend was observed in *experiment* 2, but did not reach statistical significance. Transfer of visuomotor learning, computed as the percentage of adaptive deviation at the endpoint of test reaches relative to that at the reversal of trained slicing movements, was modest in both cases (29 ± 22% in *experiment* 1 and 13 ± 16% in *experiment* 2). The amount of transfer did not differ between experiments ($P = 0.201$).

ADAPTATION AND TRANSFER DURING REACH TRAINING. With reach training (Fig. 2*D*), mean adaptive deviations of reaches compensated almost fully for the imposed 30° rotation at the end of the stabilization period without visual feedback (*experiment* 1: −28.3 ± 3.1°; *experiment* 2: −29.4 ± 2.4°). However, initial directions became more variable and hand paths became curved over the course of training. In most subjects, reaches were launched in a direction intermediate between baseline and fully adapted directions (deviation at midmovement in *experiment* 1: −20.7 ± 5.9°; *experiment* 2: −21.9 ± 2.4°), with curvatures or bends developing later in the movement or during postural stabilization (Fig. 2*D*, *middle*). Thus the curvature of hand paths for reaches (*experiment* 1: $d\theta$ = −10.2 ± 5.1°; *experiment* 2: $d\theta = -9.4 \pm 4.6°$; Fig. 3*D*) was greater in magnitude than that for slices (*experiment* 1: $d\theta$ = −3.3 ± 0.9°; *experiment* 2: $d\theta = -3.1 \pm 0.7°$; Fig. 3*D*). This difference, pooled across experiments, was highly significant ($P = 008$). Note that reach curvature after reach training was oppositely signed to reach curvature observed after slice training (see Fig. 2*C*), with the different training conditions resulting in vastly different reach curvature values (two-sample *t*-test: $P < 0.0005$). In contrast, reversal points of test slices remained unadapted (*experiment* 1: −5.8 ± 2.7°; *experiment* 2: −7.7 ± 10.1°) and straight. Transfer of rotation learning from reaching to slicing was only 19 ± 14% in *experiment* 1 and 26 ± 32% in *experiment* 2. Again, the difference in transfer between experiments was not significant ($P = 0.669$).

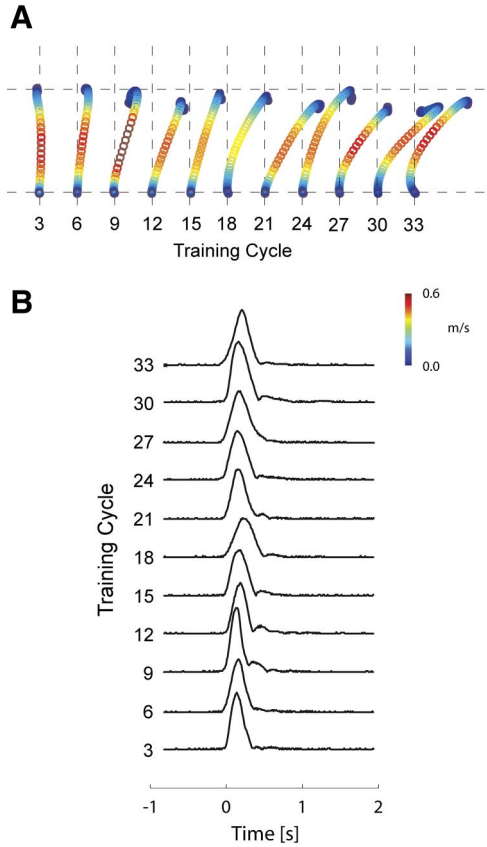

FIG. 3. Hand path curvature developed gradually during reach training. *A*: hand paths of individual trials sampled every 3 cycles of 8 movements for a representative movement direction from a representative subject. Color indicates hand speed according to the scale bar in *B*. *B*: tangential hand velocity profiles from the trajectories shown in *A*. Note that the speed profiles are predominantly unimodal and that hand path curvature develops without the presence and/or merging of corrective submovements.

ANOVA found that transfer of learned visuomotor rotations between tasks was not dependent on either the trained task [$F(1,19) = 0.00$; $P = 0.96$] or on experiment [$F(1,19) = 0.44$; $P = 0.52$]. Thus lack of transfer cannot be attributed to differences in peak speeds of reaching and slicing movement because these were large in *experiment* 1 and modest in *experiment* 2. We also found using linear regression that the amount of transfer did not correlate with speed, even in *experiment* 1 where the range of peak speeds was large.

We found no evidence suggesting that the curvature developed with reach training resulted from progressive merging of a primary movement and later correctional submovements. As shown for a representative movement direction from a representative subject (Fig. 3*A*), substantial curvature developed in the second half of training without inflections in the velocity profile (Fig. 3*B*), which would have indicated the presence of corrective submovements.

DISCRETE DIRECTION-DEPENDENT ADAPTATION. In three subjects, exposure to visuomotor rotation during reach training induced very prominent hand path curvatures, whereas reaching movements had invariably been straight during baseline practice. In contrast to the examples shown in Fig. 2*D*, maximal curvature in these subjects occurred in the middle rather than at the end of movement (Fig. 4, *middle*). This pattern was not contingent on the presence of a destabilizing environmental perturbation as it was observed in one subject in *experiment* 1 and in two subjects from *experiment* 2. The direction of curvature sometimes varied systematically for the different targets (Fig. 4*B*), although curvature was not always the same for movements to the same target. This suggests that for some targets, these subjects made a discrete categorical decision as to which of two alternative initial directions to move their hand to reach those particular targets. As with the majority of subjects, individuals demonstrating extreme curvatures acquired reach endpoints that were systematically rotated but made test slices that remained straight and unadapted (Fig. 4, *right*).

ASYMMETRIC TRANSFER OF MOVEMENT EXTENT. An unexpected observation made in *experiment* 1 was that test slices performed after reach training invariably overshot the goal on both outward and return phases of movement (see Fig. 2*D*, *right* and Fig. 4, *right*). Movements were also hypermetric in *experiment* 2, but to a lesser degree. The mean outward extent of slices increased by 26 ± 1% relative to reaches in *experiment* 1 and by 12 ± 7% in *experiment* 2 (Fig. 5). In some directions (*experiment* 1), slice extents increased as much as 37%. Paired

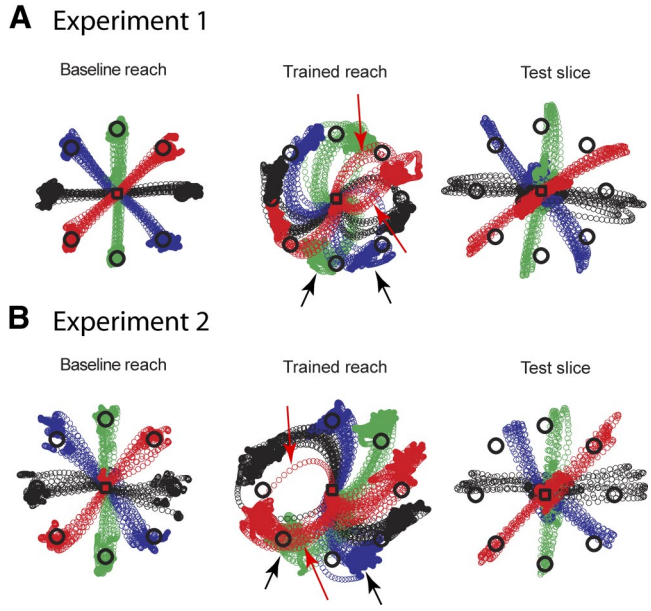

FIG. 4. A minority of subjects participating in each of the experiments had extremely curved hand paths after reach training. *A*, *experiment* 1: although hand paths of reaching movements before training were straight (*left*), reaches performed after rotation training for this subject were exceedingly curved (*middle*). Mean absolute magnitude curvature $|d\theta|$ for these movements was 21°. For some target directions, reaches could be quite variable in their initial launch directions. In contrast, slices performed after reach training were directed straight out-and-back to the target and were hypermetric in all directions. *B*, *experiment* 2: here again (for a different subject), untrained reaches were straight, whereas trained reaches had very curved hand paths and variable launch directions. Mean absolute magnitude curvature $|d\theta|$ for these movements was 46°. Slicing movements after reach training were straight as in *experiment* 1 and were hypermetric in some directions.

t-tests comparing reach and slice extents following reach training in both experiments found slice hypermetria to be significant (*experiment* 1: $P < 0.0005$; *experiment* 2: $P = 0.015$). Hypermetria was even more evident for the return phase of slicing movements, being 18 ± 5% longer than outward phases in *experiment* 1 and 19 ± 5% longer in *experiment* 2, such that the hand consistently overshot the home target on return (compare Fig. 2, *A*, *middle* and *D*, *right*). We did not attempt to determine whether hypermetria was evident earlier (e.g., at peak velocity or peak acceleration) because the effective limb inertia varies with movement direction (Hogan 1990), and our sample included only three test trials in each movement direction for each subject. This analysis was instead performed in a companion study involving a single movement direction and found that significant hypermetria was present at peak velocity, but not peak acceleration (Ghez et al. 2007; Scheidt and Ghez 2006a,b).

Separate one-way ANOVAs found that out- and return-phase slice hypermetria after *reach* training was dependent on experiment [Out: $F(1,9) = 20.02$, $P = 0.002$; Ret: $F(1,9) = 6.77$, $P = 0.031$]. Hypermetria was greater in both phases when subjects were trained to stabilize the hand against an environmental perturbation at the peripheral reach target (*experiment* 1) than when this requirement was removed. Importantly, there was no change in movement extent in untrained test reaches relative to baseline after *slice* training in either experiment.

Simulations: independent planning of trajectory and posture predict observed movement errors

Modest transfer of learning between the two movement tasks is difficult to explain by the adaptation of a unified mechanism (including an equilibrium trajectory controller) regulating both trajectory reversals and final stabilized positions according to a common spatial plan. Rather, it suggests that subjects adapted different internal representations of target location to aim movement reversals and final stabilized hand positions. In any case, the observations of reach curvature after slice training and slice hypermetria after reach training are puzzling. We therefore evaluated (using inverse and forward dynamic simulations of arm motion) whether a simple control strategy that included separate feedforward specification of the hand's initial trajectory and its final stabilized position could explain these effects heuristically. We assumed that the initial trajectory controller specifies a nominally straight hand path with a bell-shaped velocity profile (Morasso 1981), whereas the final position controller specifies a fixed, terminal equilibrium position (termed *posture point*). We further assumed that reaching movements resulted from the superimposition of both control actions. We initially assumed that the target posture points at the endpoints of reaches and at the return of slices were instantiated [i.e., $\mathbf{\Phi}(t) > 0$] at the time of peak acceleration of the outgoing and return phases of the movements, respectively. This was based on our findings of similar initial accelerations in reaching and slicing but different peak speeds as discussed earlier, although we assessed the sensitivity of the simulation predictions to variations in timing as subsequently noted. We also assumed that the equilibrium point at the reach target began to decay 250 ms after onset. We first examined the

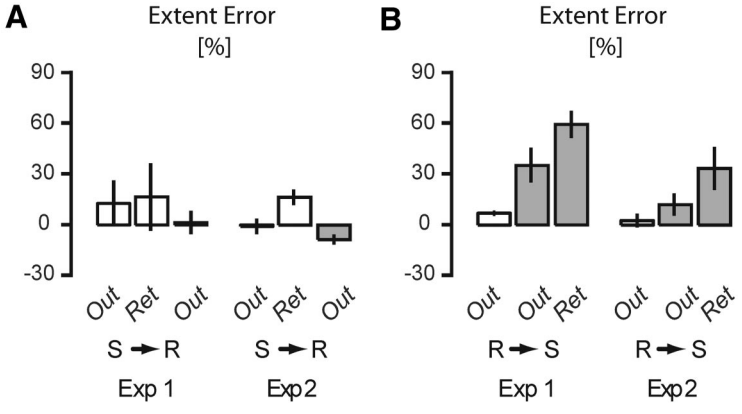

FIG. 5. Average peak (or end) hand displacements after slice training (*left*) and reach training (*right*). *A*: outward and return phases of trained slices were reasonably well calibrated to the desired movement extent in both *experiment* 1 (*left*) and *experiment* 2 (*right*). Test reaches after slice training were also well calibrated to the desired extent. *B*: whereas the extent of trained reaches were well calibrated to the desired movement extent in both experiments, test slices after reach training were hypermetric during both the outward and return phases.

sensitivity of simulated hand paths to variations in joint impedance as well as to changes in the onset and development timing of the posture point. It is important to note that this heuristic model does not examine how the motor system optimizes the linearity and smoothness of hand trajectories or how limb impedances at the posture point are optimized to achieve accuracy or stability. Nevertheless, a key assumption is that trajectories are optimized based on feedback alone, without taking into account the limb impedance that will be specified at the end of movement (i.e., for the intended posture point).

The displacement and speed profiles for a nominal 0.5-s reach are shown in Fig. 6*A*. Here we assume that the posture point Φ_R began developing at peak acceleration (see ASYMMETRIC TRANSFER OF MOVEMENT EXTENT). The *bottom traces* show the computed elbow and shoulder torques required to produce the desired displacement. Separate lines show the isolated contributions from the feedforward controller without equilibrium stabilization (black), contributions from the developing equilibrium point (gray dots), and the feedforward torques required to produce the template movement with the equilibrium point instantiated (gray). Elasticity at the posture point initially serves as an attractor, whereas joint viscosity later dissipates energy (gray dots). Therefore when stabilization is required at the reach target, the feedforward extensor torque (gray line) must be reduced initially and increased later (relative to the black line) to achieve the template trajectory, although failing to take these factors into account results in only minor terminal deviations from linearity and a modest change in the symmetry of the hand speed profile (Fig. 6*B*).

We next simulated the kinematics of slicing movements produced by feedforward torques calibrated for reaching (Fig. 6*C*). The black lines (*top traces*) show the nominal displacement and speed profiles with posture points at both reach and return (end) targets. The gray lines (Fig. 6, *C* and *D*) show that displacements are hypermetric both at the reversal and the final position if a posture point was anticipated at the reversal target in slicing but none was actually implemented. By erroneously anticipating increased joint impedance about the reach target during the slice, excess feedforward joint torques move the

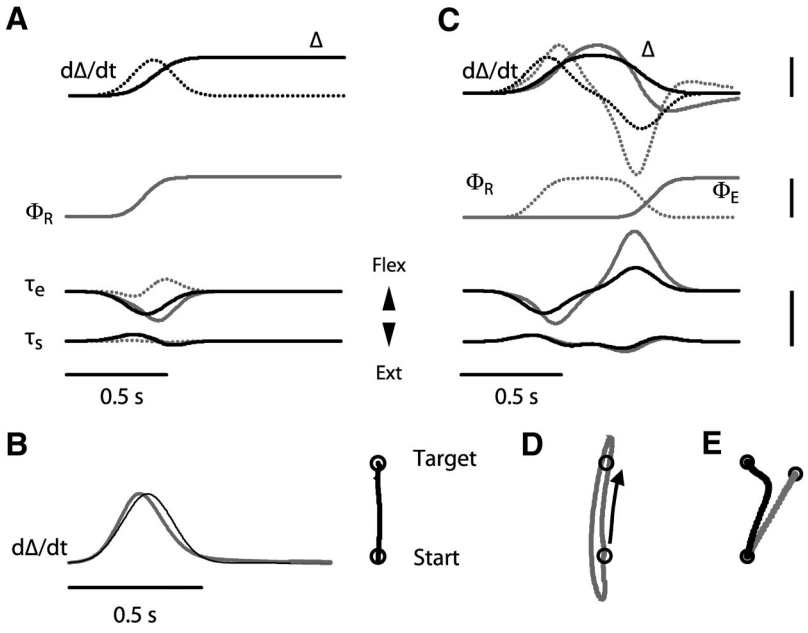

FIG. 6. Simulated movements with independent control over initial trajectory and final position. *A*: hand displacement (Δ; solid line) and speed (dΔ/dt; dashed) for an ideal, 10-cm, 0.5-s reaching movement. Φ_R is a multiplicative factor ranging from 0 to 1 that determines the time course of equilibrium point development at the fixed reach target location. Φ_R starts turning on when the outward acceleration peaks and is fully instantiated 200 ms thereafter. τ_E and τ_S are the net elbow and shoulder torques (solid black) needed to drive limb inertia through the ideal trajectory. Net torques were computed by inverse dynamics when contributions from postural stabilization were zero (i.e., B* = 0 and K* = 0). Dashed gray: additional torques needed to overcome increased limb impedance due to the presence of the equilibrium point at the reach target (the impedance torque). Impedance torques were computed by setting both viscosity (B*) and stiffness (K*) coefficients at 1.5 (within the physiological range; Gomi and Osu 1998; Lacquaniti et al. 1993). Solid gray: net torques required to produce the ideal kinematics with the equilibrium point instantiated. *B*: forward dynamic simulations of reach hand path and speed profiles made without (black) and with (gray) compensation for endpoint stabilization at the reach target. We used the unadjusted net torque of *A* (*black traces*) as feedforward drive for the simulated arm in both cases, even though the arm dynamics used in the forward simulation shown in gray included increased impedance about the reach target. Although the simulated speed profile (gray dΔ/dt trace) is asymmetric relative to the ideal (black), the predicted hand path does not deviate markedly from a straight line. *C* and *D*: simulations of slicing movements showing the consequence of overestimating limb impedance at the reach target. Presentation of time series is as in *A*, although here, 2 posture points were sometimes instantiated: Φ_R (dotted) shows the transient development of a posture point at reversal (corresponding to a trained reach), whereas Φ_E (solid) shows the development of a posture point at the end (home) target. Again, the location of these posture points was fixed in space. Black Δ, dΔ/dt, and τ traces depict a slice properly calibrated to attain the reach and return targets without postural stabilization (i.e., B* = 0 and K* = 0). Gray τ traces correspond to the condition where slicing was properly calibrated to attain the reach and return targets *with* increased limb impedance at both targets (i.e., B* = 1.5 and K* = 1.5) as might occur if the feedforward controller planned joint torques to account for the increased joint impedance experienced during reach training. Gray D and dΔ/dt traces were obtained using the gray τ traces to drive an arm model without increased impedance about the reach target. As can be seen in *D*, the predicted hand paths of outward and return movements were markedly hypermetric and somewhat curved as a result of overestimating limb impedance at the distal target when slicing. *E*: simulation of reaching with a posture point at the unadapted target location (*black trace*), using feedforward torques calibrated during the outward phase of a 30° adapted slice (*gray trace*). Scale bars indicate (from *top* to *bottom*) hand speeds of 0.5 m/s, posture point scaling from 0 to 1, and joint torques of 10 Nm.

hand beyond the target (gray, Fig. 6, *C* and *D*), replicating the hypermetria of blind slices made after reach training observed earlier. This would not have occurred had the trajectory controller correctly anticipated the impedance changes produced by relocating the requirement of terminal stabilization from peripheral to home target at the end of slicing movements.

To evaluate the sensitivity of slice hypermetria to variations in stiffness and viscosity at the posture point, we systematically varied K* and B* in a separate set of simulations (Fig. 7*A*). For values of elbow and shoulder stiffness and viscosity in the physiological range (Gomi and Osu 1998; Lacquaniti et al. 1993), the degree of hypermetria in the outward phase of simulated slices was mainly sensitive to the viscosity coefficient at the posture point. This could be partially offset by increasing joint stiffness, but at the cost of increased hypermetria of the subsequent return segment. Additional sensitivity analyses (not shown) demonstrated that these effects were the same for other nominal values of limb inertia, joint stiffness, and viscosity throughout the range of damping factors reported by Perreault and co-workers (2004) and Bennet et al. (1994) in other posture and movement tasks.

We next assessed the sensitivity of trajectory shape to variations in the relative onset time and the time course over which the posture point develops, as might occur if the two commands were not precisely coordinated. Figure 6*E* shows a simulated hand path resulting from the combination of a feedforward trajectory command aimed at 30° (simulating the outward path of an adapted slice) followed by an unadapted postural command at the time of peak acceleration. As in untrained reaching movements observed after rotated slice training (Fig. 2*A*, *right*), the hand path is initially directed in the adapted clockwise direction, and then bends toward the unadapted posture point. Variations in the time of onset of the posture point and the rate at which impedance develops influenced the amount of initial deviation and the trajectory curvature. Relatively straight initial paths and later bends are seen both with posture points instantiated at peak acceleration and peak speed (Fig. 7*B*). Deviations in initial direction and variations in curvature increase when the posture point develops more gradually (over 300 and 500 ms). Thus the appearance of partial transfer early in the movement may occur because of the superimposition of separate motor commands specifying a given initial trajectory direction and a different final position.

DISCUSSION

The present study investigated whether the hand's trajectory and its final position are controlled differentially in reaching. We asked whether learning a visuomotor rotation while moving the hand out-and-back to one of eight concentric targets (the trajectory to the reversal point in the "slicing" task) would transfer to a task that required maintaining the hand stable at these same locations (the positioning or "reaching" task) and vice versa. To isolate learning of final position from initial trajectory in the reaching task, we provided cursor feedback (spatial error information) only after the movement had ended. Transfer of learning would suggest that control of the hand's entire trajectory, including its endpoint, was guided by a single, common, spatial plan. Instead, we found minimal transfer of learning between tasks, suggesting that the brain used different representations of target position to specify the hand's trajectory and its final position. We also found unexpected asymmetrical effects of practice on hand paths, including systematic curvature of reaching movements after rotation training and hypermetria of untrained slice reversals after reach training. Both sets of observations were reproduced in forward dynamic simulations by using separate feedforward controllers, implemented sequentially, to specify the hand's initial trajectory and its final equilibrium position. These findings support the conclusions that *1*) the brain uses different mechanisms to plan the hand's initial trajectory and final position in point-to-point movements, *2*) that it implements the respective control actions sequentially, and *3*) that planning of the initial trajectory does not take account of the specific impedance values to be implemented about the final stabilized posture.

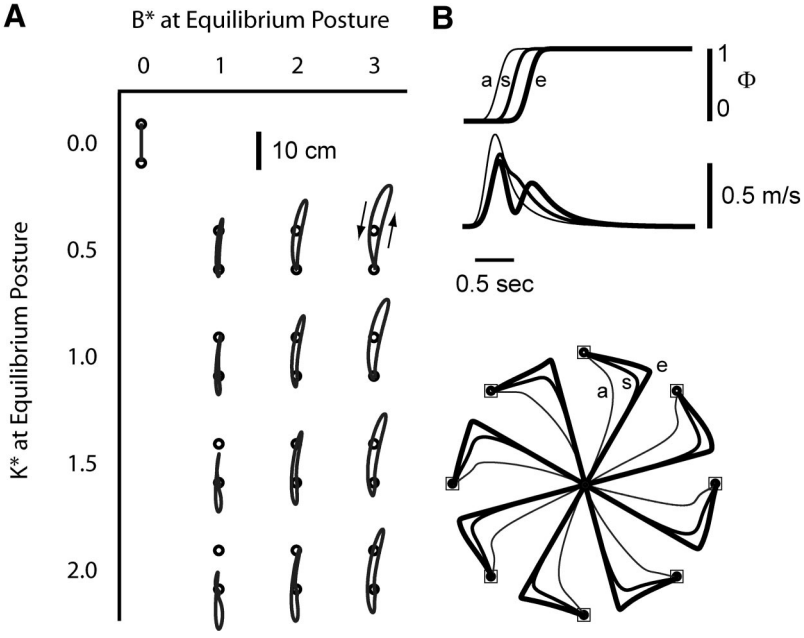

FIG. 7. *A*: sensitivity of simulated hand paths to variations in (*A*) joint stiffness and viscosity as well as to (*B*) the onset time of posture point development at reach targets. *A*: simulations were performed by using the scaling factors indicated above and to the left of each trace during inverse dynamic joint torque calculation. These torques were then used to drive a limb model that did not include a posture point at the reach target. *B*, *top*: posture point profiles with onsets at peak acceleration (a, *thin trace*), peak speed (s, *medium trace*), and at the end of movement (e, *thick trace*). *Middle*: simulated hand speed profiles for each case. *Bottom*: reach curvature is predicted regardless of posture point onset timing even though learning was isolated to the trajectory plan in these simulations.

Separate and sequential control of trajectory and final position in reaching

The finding that the arm's initial trajectory and its final stabilized position adapt differentially to imposed visuomotor rotations appears to resolve a long controversy regarding how the brain controls reaching movements. Early proposals considered that neural control might be simplified by specifying only the limb's intended final posture (Holmes 1939). The hand's trajectory would emerge due to viscoelastic restoring forces generated by the contraction of opposing muscles in the transition between controlled equilibrium positions (Asatryan and Feldman 1965; Polit and Bizzi 1978; Rosenbaum et al. 1995). Modulation of limb impedance about the endpoint of movement would serve to compensate for prediction errors by the feedforward controller, including the effects of unexpected interjoint coupling torques (Gribble and Ostry 2000). However, a large body of evidence supports the idea that the CNS instead controls trajectory kinematics explicitly. This view received strong support from studies of reaching in the horizontal plane, which demonstrated that subjects recover relatively straight and smooth hand paths in adapting to environmental perturbations (Dizio and Lackner 1995; Ghez et al. 1999; Sainburg et al. 1999; Scheidt et al. 2000; Shadmehr and Mussa-Ivaldi 1994; Thoroughman and Shadmehr 2000). Different models have been proposed to govern the entire hand trajectory from start to end, using a common spatial plan (Flanagan et al. 1993; Flash and Gurevich 1997; Gottlieb et al. 1997; Gribble and Ostry 2000; Gribble et al. 1998; Harris and Wolpert 1998; Latash and Gottlieb 1992). Such unified models should predict transfer of adaptation between slicing and reaching. Our observations did not bear this out. Learning of rotations that were compensated at the final position of reaches did not transfer to test slices, which remained straight and unadapted. Rotations learned while slicing produced modest and variable changes of unpracticed test reaches to the same targets, but were limited to the initial portions of the trajectories. The hand then curved back toward the untrained final position. Thus the trajectory required to achieve a specific reversal point was learned independently of the final planned postural equilibrium.

It might be objected that the lack of transfer in *experiment* 1 occurred because subjects in the two training groups experienced visual feedback of hand motions at very different speeds: Those undergoing reach training saw the cursor only during slow terminal adjustments, whereas those receiving slice training saw the cursor move over a much larger range of hand speeds and locations. These different feedback signals might have driven adaptation of separate components of a single controller such as that recently proposed by Hwang and colleagues (2003). In that model of motor control, second-order state-space (joint position and velocity) is tiled with adaptive modules tuned to different combinations of movement direction and speed (Hwang et al. 2003). However, this would not account for the limited transfer in *experiment* 2, wherein cursor feedback provided the same quasi-static information of hand position at reversal in slicing and at the movement endpoint in reaching. That model also would not account for the lack of transfer from slicing to reaching in *experiment* 1 because cursor motions during slicing provided error information over the entire range of hand speeds and therefore should have allowed transfer of learning to the subset of state-space modules controlling the final position of reaches. Finally, the systematic hypermetria of both outward and return phases of test slices following reach training, and the asymmetric development of reach curvatures, are outside the prediction domain of models limited to second-order limb state estimates.

The lack of transfer found here might also be trivially explained if, based on contextual cues (e.g., target shape or color as in the *experiments* 1 and 2) or on verbal instructions, subjects had invoked completely separate control strategies in the two tasks. But again, the combined observation of curvature in reaching (but not slicing) after rotation training in both tasks and of slice hypermetria after reach training would not be expected. Instead, the adaptive deviation of initial trajectories and later curvature of untrained reaches observed after slice training was reproduced in our model by superimposing an adapted trajectory controller with an unadapted positional controller and interposing a delay between them. Different hand path curvatures were replicated both by varying the time required for developing impedance at the endpoint and by varying the time at which the positional controller is superimposed on the evolving trajectory command. Taken together, our behavioral findings and simulation results indicate that visually perceived errors in final position do not constrain the entire trajectory, but selectively adjust specific component control actions in the early and later phases of the reach, respectively. Each of these control actions must be understood to operate by adjusting different constituent patterns of muscle activity that are influenced by different spatial optimizations.

Interactions between trajectory and posture control

It has been suggested that the generation of smooth rectilinear hand trajectories in horizontal planar reaching reflects an optimization process wherein the brain minimizes variability in final hand position [i.e., the minimum-variance theory of Harris and Wolpert (1998)]. However, the deviations from linearity we observed during reaching were not corrected or compensated for during training, even though our experimental manipulation was limited to a rotation of visual feedback about the hand's starting location. Thus our findings are not consistent with the idea that trajectory rectilinearity results from the minimization of terminal kinematic variability. Because no novel mechanical loads were imposed during training, curved trajectories also would not have arisen in an attempt to optimize movement kinetics. Rather, our psychophysical results and modeling contradict the idea that a common spatial plan and/or a common spatial error signal informs the feedforward specification of initial hand trajectory and the final stabilized limb position.

Most subjects adapted to the counterclockwise cursor rotations by incremental clockwise rotation in the initial direction or the final position of slicing or reaching movements, respectively. Such changes were approximately uniform for all eight targets. However, in a subpopulation of subjects training on the reaching task, adaptive adjustments were not uniform either for the different targets or even for a single target. For some, the hand sometimes approached the target from a clockwise and sometimes from a counterclockwise direction (Fig. 4, *A* and *B*, *red traces* with red arrows). For others (Fig. 4*B*, black arrows), the hand approached the target from different directions on successive trials. The bimodal distributions of the resulting

adaptive deviations allowed us to exclude these subjects from the common analysis presented earlier. The number of subjects behaving in this way was too small for us to ascertain its determinants, although it may have been encouraged by higher directional variability and the lack of visual trajectory feedback in reaching. We speculate that this behavior represents a distinct categorical or cognitive mode of adaptation (Bock et al. 2003; Ghez et al. 1997). It is nevertheless of interest in these cases that hand trajectories showed unusually high degrees of curvature, although endpoints showed levels of accuracy comparable to those of the other subjects. This stresses that terminal movement accuracy need not entail rectilinearity of hand paths.

The systematic hypermetria of both outward and return phases of slicing movements after reach training was present in all subjects and was predicted by our simulations. Sensitivity analysis showed that the magnitude of this hypermetria varied primarily with velocity-dependent resistance (viscosity) at the equilibrium position (Fig. 7*A*). We assumed that although the trajectory controller maintains nominal velocity profiles and rectilinear hand paths in its attempt to produce desired displacements, it is not specifically informed of impedance changes to be produced by the positional controller later during movement. Thus when switching from reaching to slicing, the elevated torques needed to overcome heightened viscosity at the endpoint during reach training would result in slice hypermetria that scales with the expected terminal viscosity. Consistent with this, hypermetria was greater when subjects had to counter a destabilizing perturbation (*experiment* 1) than when they did not (*experiment* 2). This suggests that, like our model, the neural trajectory planner does not account for impedance changes produced by later phases of the planned motor sequence but adapts to them in the course of practice. This may seem surprising because subjects can vary joint stiffness and viscosity while maintaining a specific limb configuration (Lacquaniti et al. 1993). However, changes in endpoint viscoelasticity depend complexly on the mechanical properties and activation levels of multiple muscles at multiple joints (Perreault et al. 2004; Zhang and Rymer 2001) as well as on the accuracy requirements of the task (Gribble et al. 2003) and may therefore be difficult to predict accurately. Whatever the explanation, our findings support the conclusion of Milner and co-workers that impedance may be controlled independently of trajectory in reaching (Burdet et al. 2001; Franklin et al. 2003; Tee et al. 2004).

It is important to note that the heuristic model we used to simulate the compound effects of separate feedforward commands specifying the intended trajectories and final positions ignored contributions of "on-line" error correction. This was justified by the fact that movements were directed by visuospatial information. Indeed, visual errors that might have been detected during flight in *experiment* 1 were not used to correct directional errors in slicing because those movements remained straight. Furthermore, visual errors were explicitly excluded from reaching movements in *experiment* 1 and movements of both types in *experiment* 2. However, proprioceptive feedback remained present in all cases. The integrity of stretch reflexes, which depends on this, is essential for the regulation of muscle properties (Nichols and Houk 1975) and joint impedance (Sanes and Shadmehr 1995; see also Houk and Rymer 1981). The final equilibrium position posited and assumed by our model depends on setting both stretch reflex thresholds and cocontraction levels as required for the desired arm configuration as has been emphasized by Feldman and co-workers (cf. Feldman 1966, 1986; Feldman and Levin 1995; Flanagan et al. 1993). Therefore the finding by Shapiro et al. (2004) that segmental reflex mechanisms in single joint movements are facilitated only after the expected time of the peak velocity is consistent with the distinction between sequential trajectory and postural control suggested here.

Why two controllers instead of one

Because the planned trajectory itself specifies a particular endpoint, use of a separate plan for the final position may appear redundant or, worse yet, a source of potential performance variability and/or error. This might be the case if both controllers were updated using the same performance error estimates. This question is addressed further in our second study (Ghez et al. 2007), which demonstrates that accurate control of trajectory direction requires accurate information about initial hand position (see also Ghilardi et al. 1995; Rossetti et al. 1995; Scheidt et al. 2005; Vindras et al. 1998), whereas control of final limb posture is significantly less sensitive to this (Ghez et al. 2004; Scheidt et al. 2004). The robustness of final position control is evident in the compensation for large variations in initial direction at movement onset (e.g., Fig. 4). It is also likely that this independent final position control provides compensation for direction-dependent variations in initial hand acceleration that might otherwise result from anisotropic limb inertia (Gordon et al. 1994; Vindras et al. 2005). Thus the secondary implementation of stiffness control about an intended final position can reduce (rather than increase) systematic and variable errors of planned trajectories. An important question for future studies will be to determine the mechanisms responsible for maintaining precise timing of sequential control actions in multijoint movements, especially for slice reversals where slight deficits in the timing of shoulder and elbow torques can lead to dramatic hand path errors. Based on the finding of Cordo and colleagues that subjects can use proprioceptive input to trigger voluntary hand opening during an elbow extension task (Bevan et al. 1994; Cordo et al. 1994), we expect the dynamic signals provided by group Ia muscle stretch receptors to play an essential role in learning the critical timing of sequential control actions necessary to achieve an accurate final goal in tasks such as reaching and slicing.

Finally, recent experimental evidence suggests that brain injuries arising from stroke in different locations in the two hemispheres can differentially impair the adaptation of reach trajectories and the regulation of final limb position (Haaland and Delaney 1981; Haaland et al. 2004; Schaefer et al. 2007; cf. Scheidt and Stoeckmann 2007). Sainburg and colleagues also found in healthy individuals that the dominant arm demonstrates a distinct advantage over the nondominant arm in controlling the effects of limb dynamics (e.g., segment inertial interactions) on movement trajectory formation (Bagesteiro and Sainburg 2002; Sainburg 2002; Sainburg and Kalakanis 2000; Sainburg et al. 1999), whereas others have found that the nondominant arm may be used preferentially in tasks where strength and stability are required (Healey et al. 1986; see also Bagesteiro and Sainburg 2003). These findings provide coincidental support for the presence of separate neural mecha-

nisms and circuitry for controlling movement and posture, as was suggested by recent neural recordings (Kurtzer et al. 2004). Separate control as proposed here would also have important implications for the design of rehabilitation strategies because approaches optimized to address postural deficits should differ from those optimized for correcting trajectory planning deficits.

ACKNOWLEDGMENTS

We thank S. Mussa-Ivaldi for valuable discussions and support during the course of these experiments.

GRANTS

This work was supported by National Science Foundation Grant BES 0238442; Whitaker Foundation Grant RG010157; and National Institutes of Health Grants R24 HD-39627, NS-022715, and NS-35673.

REFERENCES

Asatryan DG, Feldman AG. Functional tuning of nervous system with control of movement or maintenance of a steady posture—1. Mechanographic analysis of the work of the joint on execution of a postural task. *Biofizika* 10: 837–846, 1965.

Bagesteiro LB, Sainburg RL. Handedness: dominant arm advantages in control of limb dynamics. *J Neurophysiol* 88: 2408–2421, 2002.

Bagesteiro LB, Sainburg RL. Nondominant arm advantages in load compensation during rapid elbow joint movements. *J Neurophysiol* 90: 1503–1513, 2003.

Bennett D, Hollerbach J, Xu Y, Hunter I. Time-varying stiffness of human elbow joint during cyclic voluntary movement. *Exp Brain Res* 88: 433–442, 1992.

Bennett DJ. Stretch reflex responses in the human elbow joint during a voluntary movement. *J Physiol* 474: 339–351, 1994.

Bevan L, Cordo P, Carlton L, Carlton M. Proprioceptive coordination of movement sequences: discrimination of joint angle versus angular distance. *J Neurophysiol* 71: 1862–1872, 1994.

Bock O, Abeele S, Eversheim U. Human adaptation to rotated vision: interplay of a continuous and a discrete process. *Exp Brain Res* 152: 528–532, 2003.

Burdet E, Osu R, Franklin DW, Milner TE, Kawato M. The central nervous system stabilizes unstable dynamics by learning optimal impedance. *Nature* 414: 446–449, 2001.

Cordo P, Carlton L, Bevan L, Carlton M, Kerr G. Proprioceptive coordination of movement sequences: role of velocity and position information. *J Neurophysiol* 71: 1848–1861, 1994.

Dizio P, Lackner JR. Motor adaptation to Coriolis force perturbations of reaching movements: endpoint but not trajectory adaptation transfers to the nonexposed arm. *J Neurophysiol* 74: 1787–1792, 1995.

Feldman A. Functional tuning of the nervous system with control of movement or maintenance of a steady posture—II. Controllable parameters of the muscles. *Biofizika* 11: 498–508, 1966.

Feldman A. Once more on the equilibrium-point hypothesis (lambda model) for motor control. *J Motor Behav* 18: 17–34, 1986.

Feldman AG, Levin MF. The origin and use of positional frames of reference in motor control. *Behav Brain Sci* 18: 723–806, 1995.

Flanagan J, Ostry D, Feldman AG. Control of trajectory modifications in target-directed reaching. *J Mot Behav* 25: 140–152, 1993.

Flash T. The control of hand equilibrium trajectories in multi-joint arm movements. *Biol Cybern* 57: 257–274, 1987.

Flash T, Gurevich I. Models of motor adaptation and impedance control in human arm movements. In: *Self-Organization, Computational Maps and Motor Control*, edited by Morasso P, Sanguineti V. Amsterdam: Elsevier, 1997, p. 423–481.

Flash T, Hogan N. The coordination of arm movements: an experimentally confirmed mathematical model. *J Neurosci* 5: 1688–1703, 1985.

Franklin DW, Burdet E, Osu R, Kawato M, Milner TE. Functional significance of stiffness in adaptation of multijoint arm movements to stable and unstable dynamics. *Exp Brain Res* 151: 145–157, 2003.

Franklin DW, Milner TE. Adaptive control of stiffness to stabilize hand position with large loads. *Exp Brain Res* 152: 211–220, 2003.

Ghez C, Dinstein I, Cappell J, Scheidt RA. Posture and movement are encoded in different coordinate systems. *Soc Neurosci Abstr* 873.14, 2004.

Ghez C, Favilla M, Ghilardi MF, Gordon J, Bermejo R, Pullman S. Discrete and continuous planning of hand movements and isometric force trajectories. *Exp Brain Res* 115: 217–233, 1997.

Ghez C, Krakauer JW, Sainburg RL, Ghilardi M-F. Spatial representations and internal models of limb dynamics in motor learning. In: *The New Cognitive Neurosciences*, edited by Gazzaniga MS. Cambridge, MA: MIT Press, 1999, p. 501–514.

Ghez C, Scheidt RA, Heijink H. Different learned coordinate frames for planning trajectories and final positions in reaching. *J Neurophysiol* (September 5, 2007). doi:10.1152/jn.00652.2007.

Ghilardi MF, Gordon J, Ghez C. Learning a visuomotor transformation in a local area of workspace produces directional biases in other areas. *J Neurophysiol* 73: 2535–2539, 1995.

Gomi H, Osu R. Task-dependent viscoelasticity of human multijoint arm and its spatial characteristics for interaction with environments. *J Neurosci* 18: 8965–8978, 1998.

Gordon J, Ghilardi MF, Cooper SE, Ghez C. Accuracy of planar reaching movements. II. Systematic extent errors resulting from inertial anisotropy. *Exp Brain Res* 99: 112–130, 1994.

Gottlieb GL. Muscle activation patterns during two types of voluntary single-joint movement. *J Neurophysiol* 80: 1860–1867, 1998.

Gottlieb GL, Song Q, Almeida GL, Hong D-A, Corcos D. Directional control of planar human arm movement. *J Neurophysiol* 78: 2985–2998, 1997.

Gribble P, Ostry D. Compensation for loads during arm movements using equilibrium-point control. *Exp Brain Res* 135: 474–482, 2000.

Gribble PL, Mullin LI, Corthros N, Mattar A. Role of cocontraction in arm movement accuracy. *J Neurophysiol* 89: 2396–2405, 2003.

Gribble PL, Ostry D, Sanguineti V, Laboissiere R. Are complex control signals required for human arm movement? *J Neurophysiol* 79: 1409–1424, 1998.

Haaland KY, Delaney H. Motor deficits after left or right hemisphere damage due to stroke or tumor. *Neuropsychology* 19: 17–27, 1981.

Haaland KY, Prestopnik JL, Knight RT, Lee RR. Hemispheric asymmetries for kinematic and positional aspects of reaching. *Brain* 127: 1145–1158, 2004.

Harris CM, Wolpert DM. Signal-dependent noise determines motor planning. *Nature* 394: 780–784, 1998.

Healey JM, Liederman J, Geschwind N. Handedness is not a unidimensional trait. *Cortex* 22: 33–53, 1986.

Hogan N. Mechanical impedance of single- and multi-articular systems. In: *Multiple Muscle Systems: Biomechanics and Movement Organization.* New York: Springer-Verlag, 1990, p. 149–164.

Holmes G. The cerebellum of man. *Brain* 62: 1–30, 1939.

Houk JC, Rymer WZ. Neural control of muscle length and tension. In: *Handbook of Physiology. The Nervous System. Motor Control*. Bethesda, MD: Am. Physiol. Soc., 1981, sect. 1, vol. II, pt. 1, p. 257–323.

Humphrey DR. Separate cortical systems for control of joint movement and joint stiffness: reciprocal activation and coactivation of antagonist muscles. In: *Motor Control Mechanisms in Health and Disease*, edited by Zdesmedt JE. New York: Raven Press, 1983, p. 347–372.

Hwang EJ, Donchin O, Smith MA, Shadmehr R. A gain-field encoding of limb position and velocity in the internal model of arm dynamics. *PLoS Biol* 1: 209–220, 2003.

Kearney RE, Hunter IW. Dynamics of human ankle stiffness: variation with displacement amplitude. *J Biomech* 15: 747–752, 1982.

Krakauer JW, Pine ZM, Ghilardi M-F, Ghez C. Learning of visuomotor transformations for vectorial planning of reaching trajectories. *J Neurosci* 20: 8916–8924, 2000.

Kurtzer I, Herter T, Scott S. Random change in cortical load representation suggests distinct control of posture and movement. *Nat Neurosci* 8: 498–504, 2005.

Lacquaniti F, Carrozzo M, Borghese NA. Time-varying mechanical behavior of multijointed arm in man. *J Neurophysiol* 69: 1443–1464, 1993.

Latash M, Gottlieb G. Virtual trajectories of single-joint movements performed under two basic strategies. *Neuroscience* 47: 357–365, 1992.

Morasso P. Spatial control of arm movements. *Exp Brain Res* 42: 223–227, 1981.

Nichols TR, Houk JC. Improvement in linearity and regulation of stiffness that results from actions of stretch reflex. *J Neurophysiol* 39: 119–142, 1975.

Perreault EJ, Kirsch RF, Crago PE. Multijoint dynamics and postural stability of the human arm. *Exp Brain Res* 157: 507–517, 2004.

Polit A, Bizzi E. Processes controlling arm movements in monkeys. *Science* 201: 1235–1237, 1978.

Rosenbaum D, Loukopoulos L, Meulenbroek R, Vaughan F, Engelbrecht S. Planning reaches by evaluating stored postures. *Psychol Rev* 102: 28–67, 1995.

Rossetti Y, Desmurget M, Prablanc C. Vectorial coding of movement: vision, proprioception, or both? *J Neurophysiol* 74: 457–463, 1995.

Sainburg RL. Evidence for a dynamic-dominance hypothesis of handedness. *Exp Brain Res* 142: 241–258, 2002.

Sainburg RL, Ghez C, Kalakanis D. Intersegmental dynamics are controlled by sequential anticipatory, error correction, and postural mechanisms. *J Neurophysiol* 81: 1045–1056, 1999.

Sainburg RL, Kalakanis D. Differences in control of limb dynamics during dominant and nondominant arm reaching. *J Neurophysiol* 83: 2661–2675, 2000.

Sanes J, Shadmehr R. Sense of muscular effort and somesthetic afferent information in humans. *Can J Physiol Pharmacol* 73: 223–233, 1995.

Schaefer S, Haaland KY, Sainburg RL. Ipsilesional motor deficits following stroke reflect hemispheric specializations for movement control. *Brain* 130: 2146–2158, 2007.

Scheidt RA, Conditt MA, Secco EL, Mussa-Ivaldi FA. Interaction of visual and proprioceptive feedback during adaptation of human reaching movements. *J Neurophysiol* 93: 3200–3213, 2005.

Scheidt RA, Dingwell J, Mussa-Ivaldi FA. Learning to move amid uncertainty. *J Neurophysiol* 86: 971–985, 2001.

Scheidt RA, Ghez C. Asymmetric transfer of learning and systematic extent errors are predicted by independent control of trajectory and final equilibrium position in reaching. *Proc Neural Control Move Soc*, Key Biscayne, FL, 2006a.

Scheidt RA, Ghez C. Independent control of trajectory and final equilibrium position predicts asymmetric transfer of learning and systematic extent errors in reaching. *Proc 2nd Comp Motor Control Workshop*, Ben-Gurion University Negev, June 7, 2006b.

Scheidt RA, Mussa-Ivaldi F, Ghez C. Posture and movement invoke separate adaptive mechanisms. *Soc Neurosci Abstr* 873.13, 2004.

Scheidt RA, Reinkensmeyer DJ, Conditt MA, Rymer WZ, Mussa-Ivaldi FA. Persistence of motor adaptation during constrained, multi-joint, arm movements. *J Neurophysiol* 84: 853–862, 2000.

Scheidt RA, Stoeckmann T. Adaptation of reaching movements following stroke. *J Neurophysiol* 97: 2824–2836, 2007.

Shadmehr R, Mussa-Ivaldi FA. Adaptive representation of dynamics during learning of a motor task. *J Neurosci* 14: 3208–3224, 1994.

Shapiro MB, Gottlieb GL, Corcos DM. EMG responses to an unexpected load in fast movements are delayed with an increase in the expected movement time. *J Neurophysiol* 91: 2135–2147, 2004.

Soechting JF, Dufresne JR, Lacquaniti F. Time-varying properties of the myotatic response in man during some simple motor tasks. *J Neurophysiol* 46: 1226–1243, 1981.

Suminski A, Rao SM, Mosier KM, Scheidt RA. Neural and electromyographic correlates of wrist posture regulation. *J Neurophysiol* 97: 1527–1545, 2007.

Tee KP, Burdet E, Chew CM, Milner TE. A model of force and impedance in human arm movements. *Biol Cybern* 90: 368–375, 2004.

Thoroughman KA, Shadmehr R. Learning of action through adaptive combination of motor primitives. *Nature* 407: 742–747, 2000.

Vindras P, Desmurget M, Prablanc C, Vivani P. Pointing errors reflect biases in the perception of the initial hand position. *J Neurophysiol* 79: 3290–3294, 1998.

Vindras P, Desmurget M, Viviani P. Error parsing in visuomotor pointing reveals independent processing of amplitude and direction. *J Neurophysiol* 94: 1212–1224, 2005.

Zhang L-Q, Rymer WZ. Reflex and intrinsic changes induced by fatigue of human elbow extensor muscles. *J Neurophysiol* 86: 1086–1094, 2001.